Microbiol. Immunol., 47(6), 387–394, 2003

Degradation Process of *Mycobacterium leprae* Cells in Infected Tissue Examined by the Freeze-Substitution Method in Electron Microscopy

Kazunobu Amako*[,1], Akemi Takade[1], Akiko Umeda[2], Masanori Matsuoka[3], Shin-ichi Yoshida[1], and Masahiro Nakamura[4,5,†]

[1]*Department of Bacteriology, Faculty of Medical Sciences, Kyushu University, Fukuoka, Fukuoka 812–8582, Japan,* [2]*Department of Health Science, School of Medicine, Yamaguchi University, Ube, Yamaguchi 755–8505, Japan,* [3]*National Institute of Infectious Diseases, Leprosy Research Center, Higashimurayama, Tokyo 189–0002, Japan,* [4]*Koga Hospital Medical Research Lab., Kurume, Fukuoka 830–8577, Japan, and* [5]*Kurume University School of Medicine, Kurume, Fukuoka 830–0011, Japan*

Received November 14, 2002; in revised form, March 24, 2003. Accepted March 26, 2003

***Abstract*: *Mycobacterium leprae* cells (strain Thai-53) harvested from infected mouse foot pads were examined by electron microscopy using the freeze-substitution technique. The population of *M. leprae* cells from the infected tissue consisted of a large number of degraded cells and a few normal cells. These thin sectioned cell profiles could be categorized into four groups depending on the alteration of the membrane structures, and the degradation process is considered to occur in stages, namely from stages 1 to 3. These are the normal cells with an asymmetrical membrane, a seemingly normal cell but with a symmetrical membrane (stage 1), a cell possessing contracted and highly concentrated cytoplasm with a membrane (stage 2), and a cell that has lost its membrane (stage 3). The peptidoglycan layer was found to remain intact in these cell groups.**

***Key words*: *Mycobacterium leprae*, Electron microscopy, Freeze-substitution technique, Cell degradation**

Since the discovery of lepra bacillus (*Mycobacterium leprae*) as the causative agent of leprosy in 1873 by G.H. Armauer Hansen, extensive efforts have been made to culture this bacillus on artificial culture media. However, this was never successfully achieved during the 20th century. Hence, *M. leprae* for experimental uses can only be obtained from limited experimental animal tissues specimens such as those from armadillos, foot pads of nude mice or from the skin lesions of patients.

A morphological examination of *M. leprae* by electron microscopy has also been carried out on the bacteria obtained from these tissue specimens and a few normal bacteria were thus found among many of the degraded bacterial cells (7, 13, 14, 21, 23). Examinations by light microscopy also showed many dead *M. leprae* cells in the infected tissue specimens. Palomino et al. (18), using fluorescence staining technique, estimated the rate of viable bacterial cells in tissue from patients to range between 40–60%. Likewise David et al. (6) showed dead cells make up about 70% of all cells in tissue specimens from these patients by staining with fluorescence dyes. The morphological index (MI) (22) used to estimate the ratio of viable cells in tissue specimens from either *M. leprae* infected patients or animals indicated a high rate of degraded cells. This finding contrasted greatly to that of an infection of other mycobacterium where only a small percentage of dead cells were found in infected tissue specimens (21). The reason why such a large number of *M. leprae* cells in tissue are either in a nonviable or degenerating state remains to be elucidated. Silva et al. (24) described the possibility that these bacteria are killed by the action of macrophages or other phagocytes in untreated patients as well as due to the effects of drugs in treated patients. On the other hand, David and Rastogi (7) showed the cell wall of *M. leprae* to have a more fragile nature than in other bacteria. To obtain reliable data on the morphology of *M. leprae* improvements in the fixation technique for electron microscopy have been reported to be critically important (26).

It is now generally accepted that the freeze-substitution

**Address correspondence to* Dr. Kazunobu Amako, 6–19–19 Hiikawa, Jonan-ku, Fukuoka, Fukuoka 814–0153, Japan. Fax: 092–871–7776. E-mail: amako@mxw.mesh.ne.jp (Present address).

† Deceased on Feb. 2002.

Abbreviation: PG, peptidoglycan.

technique in electron microscopy is the most reliable technique to reveal fine bacterial structures in their natural states (9). Since the first application of this technique to the bacterial structure in 1983 (2), many new features of bacterial cell structures (3, 10, 12, 16, 28), including the cell wall structures of mycobacterial species (19, 20), have been reported. In this experiment we utilized this technique to examine the structure of *M. leprae* grown in the foot pads of infected nude mice and also discussed the biological meaning of the degenerative forms of *M. leprae* cells, based on newly obtained morphological findings.

Materials and Methods

Preparation of M. leprae *from an infected mouse foot pad.* The Thai-53 strain, propagated and serially maintained in nude mice (BALB/c nu/nu) foot pads, was used throughout this study. The mice were inoculated with about 1×10^6 cells of *M. leprae* in both foot pads. After 3 to 12 months, the mice were sacrificed for the experiments. Two or six foot pads were used in one experiment. A suspension of *M. leprae* was made from the foot pads as previously described (17). Briefly, the infected foot pads were minced with scissors and then homogenized using a glass homogenizer in 0.05 M phosphate buffer (PBS, pH 7.0). After removing any coarse tissue debris by low speed centrifugation ($10\times g$, for 2 min), the suspension was treated with trypsin (final 0.05% w/v, Sigma Chemical Co., St. Louis, Mo., U.S.A.) for 60 min at 37 C. After centrifugation at 2,500 $\times g$ for 30 min, the pellet was used for morphological examination.

Electron microscopy. The method for freeze-substitution fixation was essentially the same as that described previously (2, 28). The bacterial pellet was mixed with a small amount of melted (48 C) 3% noble agar and soon spread on a fresh clean glass slide. Next, the bacteria packed in agar on the glass slide were cut into small (2–3 mm^3) blocks and applied to the end of a plunger for impact freezing. The machine used for impact freezing was the KF-80 model manufactured by Reichert-Jung Optische Werk (Austria) and liquid nitrogen was used as a cryogen (−196 C). Substitution fixation was performed in acetone or ethanol containing 0.5% OsO_4 at −80 C (in a mixture of acetone and dry ice) for more than 20 hr. After raising the temperature gradually to room temperature, the specimens were then dehydrated in a series of graded acetone baths and embedded in an Epon mixture of Spurr. Thin sections

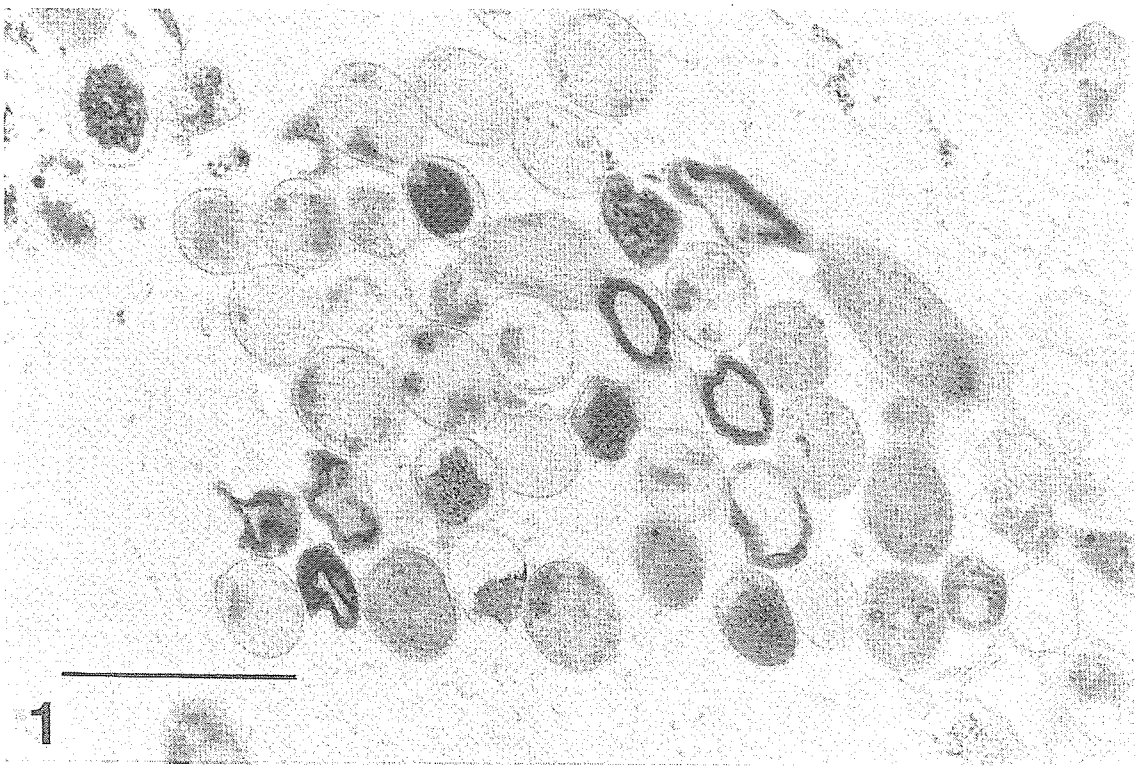

Fig. 1. A low magnification view of thin sectioned *M. leprae* from an infected mouse processed by the freeze-substitution method. Over fifty cell profiles are seen in this section and most of them show cytoplasm with a low electron density. Only a few cells exhibit a granular viable cell morphology. The scale bar is 1 μm.

were cut with a Sorval Ultramicrotome MT2 (Ivan Sorval) using a diamond knife. The thin sections were stained first with uranyl acetate followed by lead citrate, and then were examined by electron microscopy (JEM 2000EX, JEOL) at 60 kV.

Results

An electron microscopic examination of the *M. leprae* cells at low magnification revealed a variety of cell profiles as shown in Fig. 1. The majority of cell populations were degraded cells and only a few normal cells were found. In addition, the cell profiles of the degraded *M. leprae* cells were not the same. We were able to categorize these cells into several cell types; namely cells with a granular electron dense cytoplasm, cells with an electron less dense cytoplasm and cells with an electron dense but shrunk cytoplasm. These degenerated cell profiles were found in bacterial preparations isolated either in the middle stage of infection (6 months) or in late stage (12 months). At a very early stage of infection (3 months) the number of *M. leprae* cells recovered from the foot pad was not sufficient to be examined by electron microscopy. The fine structures of these cells are shown in the following micrographs at high magnification.

Figure 2 is an example of a thin sectioned profile of a *M. leprae* cell that showed the morphology of a viable cell. There are many ribosome particles in the electron dense cytoplasm and the nucleoid was not condensed centrally in the cell. The cell envelope consisted of two electron dense bands. These bands can be more clearly identified in an enlarged micrograph of the cell envelope in the inset of Fig. 2. The morphology of the cell envelope basically resembles that of other reported mycobacterial species (19). The two bands seemed to represent the peptidoglycan layer (PG) and the cytoplasmic membrane, respectively. The inner leaflet of the unit membrane of the cytoplasmic membrane did not stain intensively, hence it considered to be an asymmetrical feature by other researchers (19, 25, 26).

Figure 3 was another cell exhibiting the same cell morphology as that of the viable cell in Fig. 2, but it could be differentiated by the presence of a symmetrical membrane structure. There was a large space between the PG layer and the membrane. The nucleoid was condensed within the cytoplasm and it consisted of intertwined DNA fibers. These two micrographs revealed that

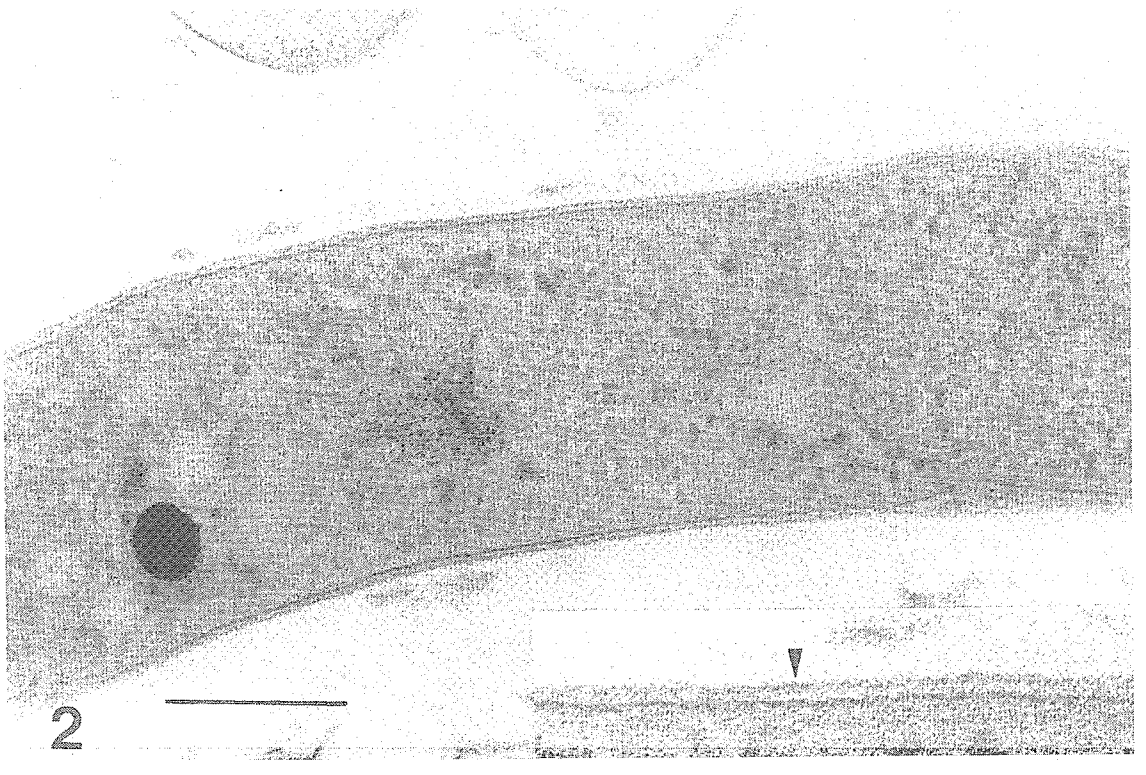

Fig. 2. Thin sectioned profile of a cell of *M. leprae* with normal viable cell morphology. Cytoplasm contains many ribosomes. The cell envelope consists of two electron dense bands which represent the peptidoglycan layer and the membrane. The inset shows an enlarged image of a part of the cell envelope showing a peptidoglycan layer (arrow head) and an asymmetrical membrane. The scale bar is 200 nm. The inset is 300,000 ×.

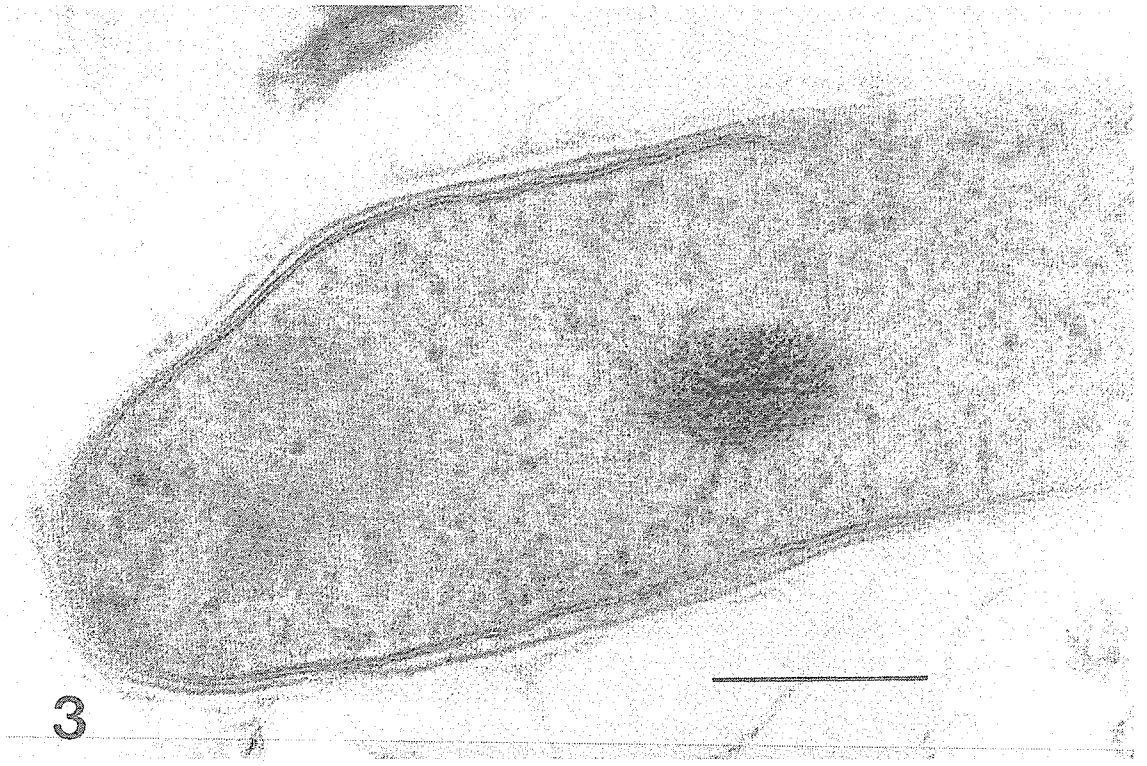

Fig. 3. Another type of cell with a viable cell morphology but a symmetric membrane. The cell membrane shows symmetric lines. There is a large gap between the PG layer and the membrane. The nucleoid is concentrated in the middle of the cells as an electron dense mass of fibrous material. The scale bar is 200 nm.

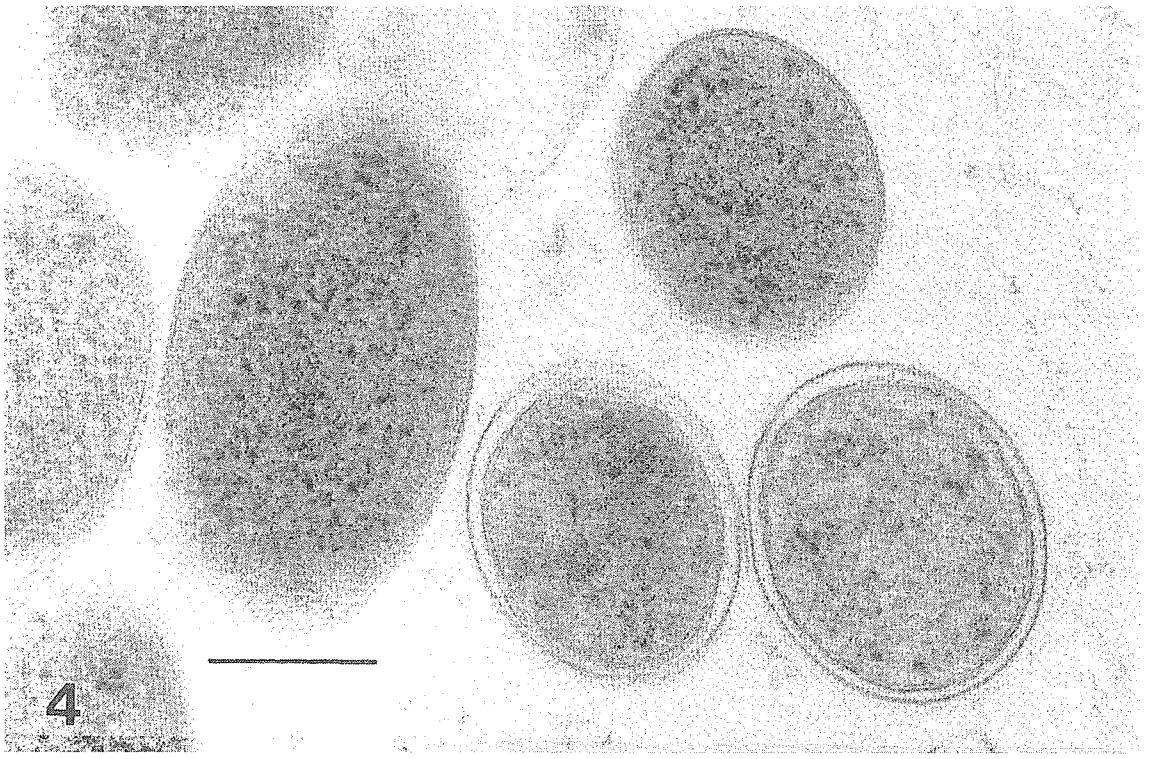

Fig. 4. Cross sections of normal looking cells and cells having symmetric membrane structure. The scale bar is 200 nm.

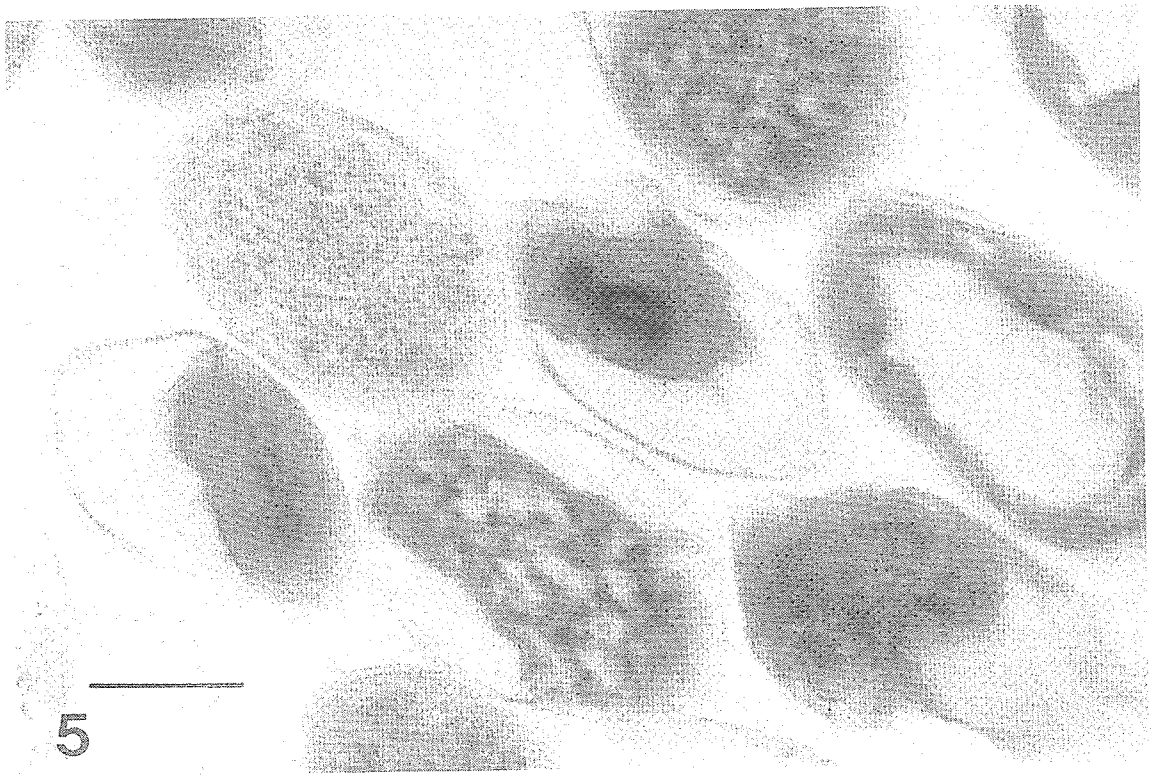

Fig. 5. One type of degenerating cell. The cytoplasm shows extensive shrinkage and an increase in density. However, the cells still have a membrane with a symmetric structure and a round shaped PG layer. The scale bar is 200 nm.

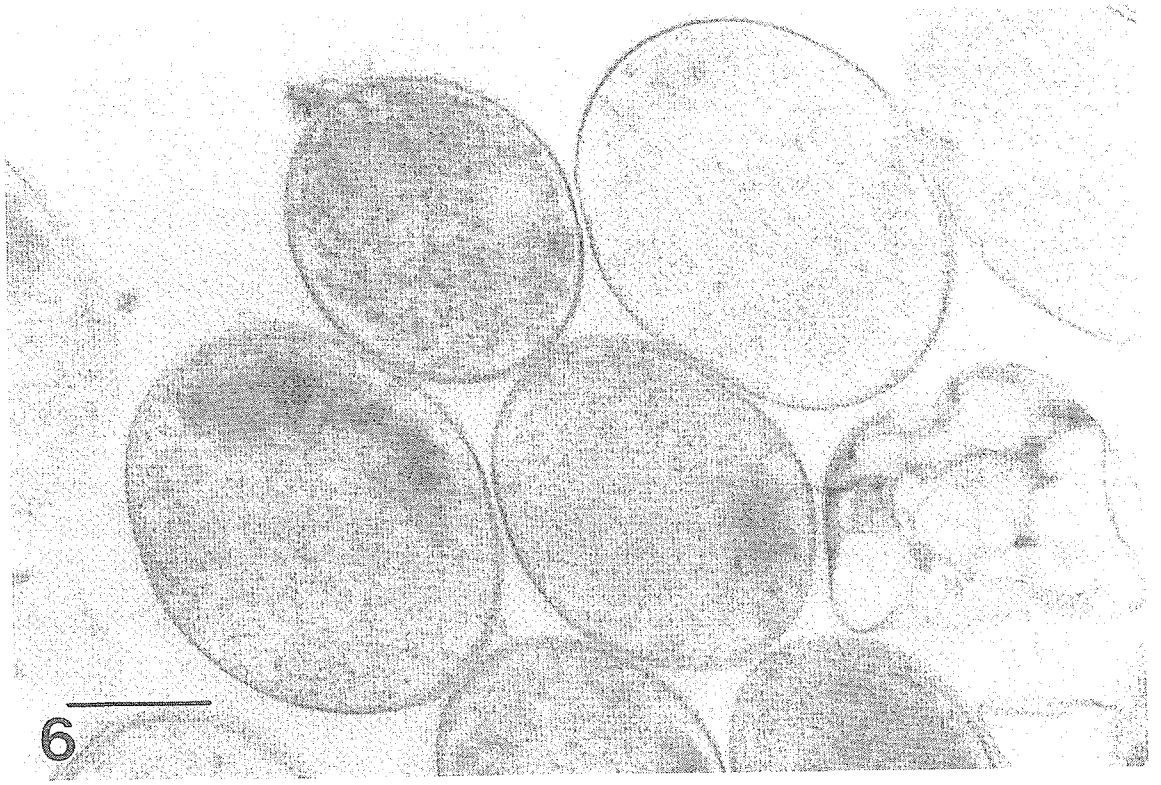

Fig. 6. Another type of degenerating cell. The membrane has disappeared. The PG layer still remains intact and the cell has kept its round shape. The cytoplasm has become less electron dense. The scale bar is 200 nm.

there were two types in structure of the cytoplasmic membrane among the cells exhibiting a granular cytoplasm with the appearance of viable cell morphology. In Fig. 4, these two types of cells are shown in cross-section in the same micrograph for comparison purposes.

Many of the other remaining cells showed either a less dense cytoplasm or a highly concentrated cytoplasm, thus indicating cells undergoing a degenerative alteration. Based on examinations under high magnification, it was possible to group these cells into two types of degradation stages. (Figs. 5 and 6)

Figure 5 showed one type of degraded cell which characteristically has a highly condensed cytoplasm but still has a cytoplasmic membrane. The other type of degenerating cell is shown in Fig. 6. In this type, the density of the cytoplasm is greatly reduced while the membrane has disappeared.

A common feature found in all of these degraded cells is the presence of a rigid PG layer which maintains a round or rod-like cell shape in bacterial cells even after the loss of most of the cytoplasmic material. Therefore, it can be assumed that the PG layer of *M. leprae* is not removed from cell population by the action of autolytic enzymes.

Discussion

Many electron microscopic observations have been made on *M. leprae* infected tissues specimens from human and animals by the conventional chemical fixation method, and all results show the presence of many degraded cells in such tissues (7, 13, 14, 21, 23). However, the conventional chemical fixation method has limitations in its ability to reveal very delicate morphological changes of the intracellular structures of the bacteria. In this experiment this morphological feature of *M. leprae* cells was examined by the freeze-substitution technique using electron microscopy. The excellence of this technique in preserving the bacterial fine structures has already been established (9). As a result, the morphological findings of *M. leprae* infected tissues obtained in this experiment are not artifacts due to preparation problems related to electron microscopy, but are very natural morphological features of this bacterium.

We confirmed the presence of the many cells with degenerative alterations in *M. leprae* infected tissue specimens using this technique. A few normal cells found among them showed cell structures very similar to other mycobacterial species reported (19).

In addition to these viable cells with a granular cytoplasm, we also found a similar cell that showed a cytoplasmic membrane with a symmetrical profile. This type of cell differs from the normal viable cell shown in Fig. 2, since it has a large space or gap between the membrane and the PG layer. Since a symmetrical membrane is thought to be an indication of degradation or damage in the membrane (25), we interpreted that these cells with symmetrical membranes represent a very early stage of cell degradation. We further infer that the gap between the membrane and the PG layer is due to the shrinkage of cytoplasm resulting from the loss of cytoplasmic materials through the degraded membrane (symmetrical membrane). We, therefore, categorized this type of cell as stage 1 of the degradation process. The presence of a concentrated nucleoid found in this type of cell may be another indication that the cell is not in a normal state (3).

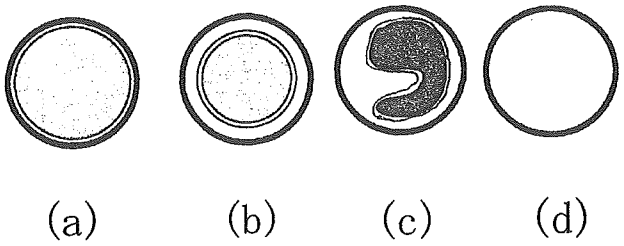

Fig. 7. The likely sequence of the cell degenerating process of *M. leprae*, deduced from thin sectioned profiles made by freeze-substitution. (a): Viable cell. (b): Stage 1. The formation of a symmetric membrane and the creation of a gap between the PG and the membrane. (c): Stage 2. Shrinkage of cytoplasm and condensation of cytoplasmic material. (d): Stage 3. The disappearance of the membrane and the diffusion of the cytoplasm through the PG layer. The PG layer apparently remains intact.

The remaining cells were highly degraded cells and made up a majority of the cell population in infected tissue. A detailed examination of these degenerating cells revealed that they could be separated into two major morphological types, one type with concentrated cytoplasm encompassed by a symmetrical unit membrane (Fig. 5) and the other having a less-dense cytoplasm without a membrane (Fig. 6).

We would like to propose a likely sequence of cell degradation from these morphological data. First, the membrane experiences some damage (stage 1), subsequently shrinkage of the cytoplasm soon occurs (stage 2) and finally the membrane disintegrates and disappears followed by a loss of cytoplasmic material (stage 3). This sequential event is summarized and illustrated in Fig. 7. On several micrographs taken (353 cell profiles) we counted the number of the viable cells. The proportion of viable cells was 17.5% (cell count: 62).

As the degradation of the cells was found in the bacteria harvested both in the middle stage of infection (6 months) and in later stage (12 months), this was not a phenomenon that particularly occurred in the late stages

of bacteria growth. We also did not embrace the idea that some bacteria from infected tissue might be killed during the preparation. The preparation method we employed is generally utilized as a mild preparation method in lepra experiments, and the morphological data so far reported have definitely suggested that the degraded cells were already present in infected tissue.

In the case of bacterial death, the autolysins are usually activated and the dead cells are eliminated from the population (15). In *M. leprae* cells, however, the PG layer remained in its original shape and therefore the dead cells are not eliminated from tissues.

The reasons why such degradation occurs in *M. leprae* cells are still not well understood, but the following possibilities can be hypothesized. One is death due to defects in the cell division mechanism. The second is death due to an insufficiency of essential nutrients for growth in a limited space of infected tissue of a foot pad.

In the last few years the phenomenon of spontaneous cell death by mutated bacteria due to an incomplete separation of chromosome during cell division has been reported (4, 11). The DNA sequence of the whole genome of *M. leprae* has been determined by Cole et al. (5) and the possibility that massive gene decay has occurred in the chromosomes of *M. leprae* was proposed, based on comparisons to the genome of *M. tuberculosis*. Therefore it is likely that *M. leprae* has some defects in its chromosomal separation machinery. If that is the case, then an incomplete separation of the chromosome during *M. leprae* cell division may result in the observed type of cell death.

Truman and Krahenbuhl (27) examined the viability of *M. leprae* in mouse foot pads using a chemical assay technique and thus showed that more of the bacteria can survive in the early stages than in the late stage of infection. This finding suggests that some unfavorable conditions for the growth of *M. leprae* may appear in the late stages of infection. In addition, Dhople (8) reported the presence of some factors that may influence the *in vivo* growth of *M. leprae* in armadillo tissue but not in mouse tissue. The capacity of the bacteria to kill themselves (suicide) after experiencing some degree of stress has now been reported (1). It is also very interesting to note that in some bacterial species a phenomenon called altruistic suicide has also been described (15). It is therefore possible that *M. leprae* may also undergo altruistic suicide as well.

In conclusion, *M. leprae* show a unique growth process. During *M. leprae* growth, a significant portion of replicating cells enter either degradation or death processes spontaneously, and consequently the population of *M. leprae* always consist of many degraded cells and few viable cells. This low percentage of viable cells in infected tissue may explain the low infectivity of *M. leprae* and the difficulty maintain such a culture in artificial media.

We thank Dr. B. Quinn for his helpful comments on the manuscript.

References

1) Aldsworth, T.G., Sharman, R.L., and Dodd, C.E.R. 1999. Bacterial suicide through stress. Cell. Mol. Life Sci. **56**: 378–383.
2) Amako, K., Murata, K., and Umeda, A. 1983. Structure of the envelope of *Escherichia coli* observed by the rapid-freezing and substitution fixation method. Microbiol. Immunol. **27**: 95–99.
3) Amako, K., and Takade, A. 1985. The fine structure of *Bacillus subtilis* revealed by the rapid-freezing and substitution fixation method. J. Electron Microsc. **34**: 13–17.
4) Britton, R.A., and Grossman, A.D. 1999. Synthetic lethal phenotypes caused by mutations affecting chromosomal partitioning in *Bacillus subtilis*. J. Bacteriol. **181**: 5860–5864.
5) Cole, S.T., Eiglmeier, K., Parkhill, J., James, K.D., Thomson, N.R., Wheeler, P.R., Honore, N., Garnier, T., Churcher, C., Harris, D., Mungall, K., Basham, D., Brown, D., Chillingworth, T., Connor, R., Davies, R.M., Devlin, K., Duthoy, S., Feltwell, T., Fraser, A., Hamilin, N., Holroyd, S., Hornsby, T., Jagels, K., Lacroix, C., Maclean, J., Moule, S., Murphy, L., Oliver, K., Quail, M.A., Rajandream, M.A., Rutherford, K.M., Rutter, S., Seeger, K., Simon, S., Simmonds, M., Skelton, J., Squares, R., Squares, S., Stevens, K., Taylor, K., Whitehead, S., Woodward, J.R., and Barrell, B.G. 2001. Massive gene decay in the liprosy bacillus. Nature **409**: 1007–1011.
6) David, H.L., Rastogi, N., Frehel, C., and Gheorghiu, M. 1982. Reduction of potassium tellurite and ATP content in *Mycobacterium leprae*. Ann. Microbiol. (Inst. Pasteur) **133B**: 129–139.
7) David, H.L., and Rastogi, N. 1983. Partial characterization of the cell wall of *Mycobacterium leprae*. Curr. Microbiol. **9**: 269–274.
8) Dhople, A.M. 1998. Factors influencing the *in vitro* growth of *Mycobacterium leprae*: effect of inoculum. Microbios **94**: 103–112.
9) Graham, L.L., and Beveridge, T.J. 1990. Evaluation of freeze-substitution and conventional embedding protocols for routine electron microscopic processing of eubacteria. J. Bacteriol. **172**: 2141–2149.
10) Graham, L.L., Harris, D., Villiger, W., and Beveridge, T.J. 1991. Freeze-substitution of gram-negative eubacteria: general cell morphology and envelope profiles. J. Bacteriol. **173**: 1623–1633.
11) Hendricks, E.C., Szerlong, H., Hill, T., and Kuempel, P. 2000. Cell division, guillotining of dimer chromosomes and SOS induction in resolution mutants (*dif*, *xerC* and *xerD*) of *Escherichia coli*. Mol. Microbiol. **36**: 973–981.
12) Hobot, J.A., Carlemalm, E., Villiger, W., and Kellenberger, E. 1984. Periplasmic gel: new concept resulting from the reinvestigation of bacterial cell envelope ultrastructure by new

methods. J. Bacteriol. **160**: 143–152.
13) Imaeda, T., and Convit, J. 1962. Electron microscope study of *Mycobacterium leprae* and its environment in a vesicular leprous lesion. J. Bacteriol. **83**: 43–52.
14) Imaeda, T. 1965. Electron microsopy in Leprosy research. Int. J. Leprosy **33**: 669–688.
15) Lewis, K. 2000. Programmed death in bacteria. Microbiol. Mol. Biol. Rev. **64**: 503–514.
16) Meno, Y., and Amako, K. 1990. Morphological evidence for the penetration of anti-O antibody through the capsule of *Klebsiella pneumoniae*. Infect. Immun. **58**: 1421–1428.
17) Nakamura, M., and Matsuoka, M. 2000. Limited ATP generation in cells of *Mycobacterium leprae* Thai-53 strain in enriched Kirchner liquid medium containing adenosine. Int. J. Leprosy **69**: 13–20.
18) Palomino, J.C., Falconi, E., and Marin, D. 1991. Assessing the viability of *Mycobacterium leprae* by the fluorescein diacetate/ethidium bromide staining technique. Indian J. Leprosy **63**: 203–208.
19) Paul, T.R., and Beveridge, T.J. 1992. Reevaluation of envelope profiles and cytoplasmic ultrastructure of Mycobacteria processed by conventional embedding and freeze-substitution protocols. J. Bacteriol. **174**: 6508–6517.
20) Paul, T.R., and Beveridge, T.J. 1994. Preservation of surface lipids and determination of ultrastructure of *Mycobacterium kansasii* by freeze-substitution. Infect. Immun. **62**: 1542–1550.
21) Rastogi, N., Frehel, C., Ryter, A., and David, H.L. 1982. Comparative ultrastructure of *Mycobacterium leprae* and *M. avium* grown in experimental host. Ann. Microbiol. (Inst. Pasteur) **133B**: 109–128.
22) Rees, R.J., and Valentine, R.C. 1964. The submicroscopical structure of *Mycobaterium leprae*. I. Application of quantitative electron microscopy to the study of *M. lepraemurium* and *M. leprae*, p.36–40. *In* Cochrane, R.G., and Davey, T.F. (eds), Leprosy in theory and practice, John Wright & Sons, Bristol.
23) Silva, M.T., and Macedo, P.M. 1982. Ultrastructure of *Mycobacterium leprae* and other acid-fact bacteria as influenced by fixation conditions. Ann. Microbiol. (Inst. Pasteur) **133B**: 59–73 .
24) Silva, M.T., Macedo, P.M., Costa, M.H.L., Goncalves, H., Torgal, J., and David, H.L. 1982. Ultrastructural alterations of *Mycobacterium lepare* in skin biopsies of untreated and treated lepromatous patients. Ann. Microbiol. (Inst. Pasteur) **133B**: 75–92.
25) Silva, M.T., Portaels, F., and Macedo, P.M. 1989. New data on the ultrastructure of the membrane of *Mycobacterium leprae*. Int. J. Leprosy **57**: 54–64.
26) Silva, M.T. 1990. Pitfalls in the ultrastructural analysis of mycobacteria, including *Mycobacterium leprae*. Trop. Med. Parasitol. **41**: 339–340.
27) Truman, R.W., and Krahenbuhl, J.L. 2001. Viable *M. leprae* as a research reagent. Int. J. Leprosy **69**: 1–12.
28) Umeda, A., Ueki, Y., and Amako, K. 1987. Structure of the *Staphylococcus aureus* cell wall determined by the freeze-substitution method. J. Bacteriol. **169**: 2482–2487.

INTERNATIONAL JOURNAL OF LEPROSY

Volume 71, Number 3
Printed in the U.S.A.
(ISSN 0148-916X)

A Second Case of Multidrug-resistant *Mycobacterium leprae* Isolated from a Japanese Patient with Relapsed Lepromatous Leprosy[1]

Masanori Matsuoka, Yoshiko Kashiwabara, Zhang Liangfen, Masamichi Goto, and Shin-ichi Kitajima[2]

ABSTRACT

Emergence of drug resistant strains of *Mycobacterium leprae* was reported soon after the introduction of dapsone (diamino-diphenyl sulphone, DDS) for leprosy treatment ([6, 10, 11]). Three cases of multidrug-resistant strains of *M. leprae* have been reported recently ([2, 8, 9, 13]). In order to prevent multiple drug resistant strains of *M. leprae* from developing, current leprosy control strategies are based on early detection of cases and treatment with multidrug therapy (MDT) as recommended by the World Health Organization (WHO). We report here the identification of a multidrug-resistant strain of *M. leprae* from a patient who received inadequate therapy for leprosy. The drug resistant profile of the isolated strain was confirmed by the mouse footpad method and the identification of mutations in genes previously shown to be associated with resistance to each drug was made.

RÉSUMÉ

L'émergence de souches de *Mycobacterium leprae* résistantes aux antibiotiques fut rapportée rapidement après l'introduction de la dapsone (diamino-diphenyl sulphone, DDS) pour le traitement de la lèpre (6, 10, 11). Trois cas de souches de *M. leprae* résistantes à plusieurs antibiotiques ont été récemment publiés (1, 8, 9, 13). Afin de prévenir l'émergence de souches de *M. leprae* poly-résistantes, l'approche actuelle du contrôle de la lèpre repose sur la détection précoce des cas et sur une poly-chimiothérapie (PCT) qui suit les recommandations de l'Organisation Mondiale de la Santé (OMS). Nous rapportons ici l'identification d'une souche poly-résistante de *M. leprae* provenant d'un patient qui a eu un traitement inadéquat contre la lèpre. Le profil de chimiorésistance de la souche isolée fut confirmé par la méthode de la plante des pieds de la souris et l'identification effective des gènes qui ont été démontré comme associés à la chimiorésistance spécifique de chaque antibiotique.

RESUMEN

Poco después de la introducción de la dapsona (diamino-difenil sulfona, DDS) para el tratamiento de la lepra aparecieron los primeros reportes sobre la emergencia de cepas de *Mycobacterium leprae* resistentes a la droga. Recientemente se han publicado tres casos de cepas de *M. leprae* con resistencia múltiple a las drogas antileprosas. Para prevenir el desarrollo de cepas de *M. leprae* multidrogo-resistentes las estrategias actuales de control de la lepra se basan en la detección temprana de los casos y el tratamiento con poliquimioterapia (PQT) como se ha recomendado por la Organización Mundial de la Salud (OMS). En este artículo describimos el caso de una cepa de *M. leprae* multidrogo-resistente derivada de un paciente que recibió un tratamiento inadecuado de la lepra. El perfil de drogo-resistencia de la cepa aislada se confirmó en el modelo de la almohadilla plantar del ratón y por la identificación de mutaciones en los genes asociados con la resistencia a cada droga.

[1]Received for publication 12 December 2002. Accepted for publication 13 May 2003.

[2]Matsuoka, M.D.V.D., Ph.D., Kashiwabara, Y., Ph. D., Liangfen, Z., M.D., Ph.D., Leprosy Research Center, National Institute of Infectious Diseases. 4-2-1, Aobacho, Higashimurayama, Tokyo, 189-0002, Japan; Goto, M., M.D., Ph.D., Second Department of Pathology, Faculty of Medicine, Kagoshima University, 8-35-1, Sakuragaoka, Kagoshima, 890-8520 Japan; Kitajima, S., M.D., Ph.D., Division of Surgical Pathology, Kagoshima University Hospital, Faculty of Medicine, Kagoshima University 8-35-1, Sakuragaoka, Kagoshima, 890-8520 Japan.
Reprint request to: Dr. M. Matsuoka at the above address or e-mail matsuoka@nih.go.jp

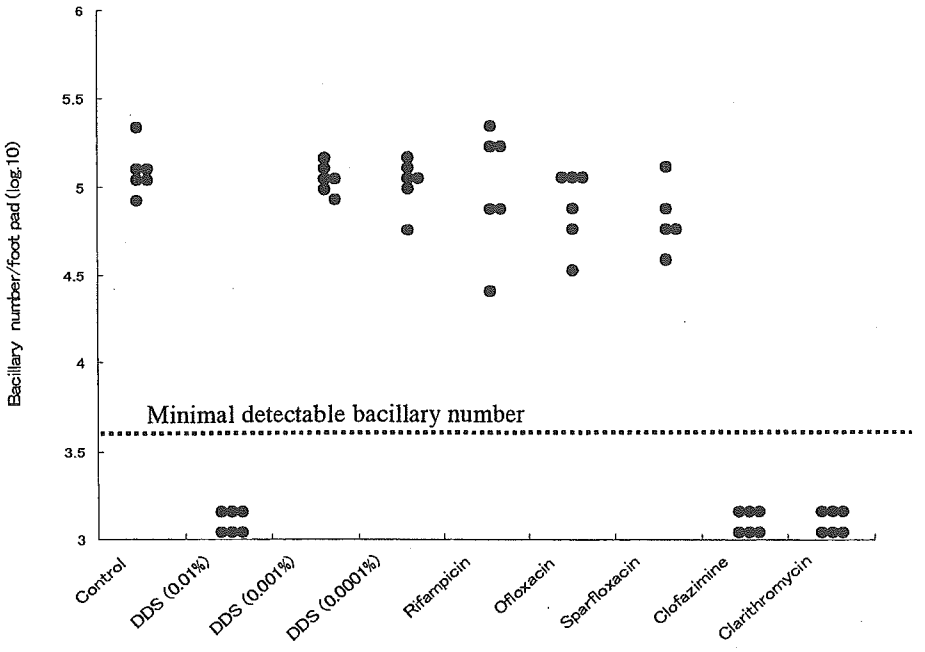

THE FIGURE. Bacillary growth in the foot pad of mice administered anti-leprosy drugs.

A 78-year old, male Japanese patient with leprosy was suspected of harboring drug resistant *Mycobacterium leprae* as a result of repeated clinical relapses. The patient was diagnosed with lepromatous leprosy (LL) and admitted to the National leprosarium at 31 years of age. The patient was first treated with promin 5 ml/day followed by dapsone 75 to 50 mg/day resulting in regression of skin lesions within one year. The patient's first relapse occurred at 50 years of age. Since the initial relapse, the patient has experienced repeated clinical relapses. During the most recent relapse, a biopsy was taken from a dermal nodule for this study. Since the initial relapse, dapsone, streptomycin, rifampicin, clofazimine, isoniazid, ofloxacin, and prothionamide were administered to treat subsequent relapses. These drugs were administered irregularly as monotherapy or in various combinations, often at doses below recommended levels, and standard multidrug therapy (MDT) was never applied.

The anti-leprosy drug susceptibility of the *M. leprae* was examined by mouse footpad method ([9]); the inoculum for footpad studies was prepared from the biopsy sample by propagating *M. leprae* in the footpads of nude mice. After expansion, *M. leprae* were tested for susceptibility to various drugs in BALB/c mice. Mice were fed standard pellet mouse chow with or without drugs, as reported previously ([9]). Experimental groups were fed diets containing one of the following drugs: dapsone, rifampicin, ofloxacin, sparfloxacin, clarithromycin, or clofazimine. Bacillary growth in each footpad was observed individually, according to the standard techniques 30 weeks after inoculation ([12]). Genomic DNA was prepared from the biopsy material to assess mutations in the *rpoβ, folP* and *gyrA* genes. DNA fragments were amplified that corresponded to regions of *rpoβ* (381-bp), *folP* (350-bp) and *gyrA* (390-bp) containing mutations, if present, associated with resistance to the rifampin, dapsone, and fluoroquinolones, respectively. Nucleotide sequences of the DNA fragments were determined by direct sequencing and analyzed by the DNASIS program, as described previously ([8]).

Bacillary growth in footpads treated with rifampicin, ofloxacin, sparfloxacin, and dapsone at concentrations of 0.0001% and 0.001% showed almost the same level of growth as seen in control mice. No bacillary growth was observed in footpads of mice treated with clarithromycin, clofazimine, and dapsone at the concentration of 0.01% (The Figure). Based on the mouse footpad method, the *M. leprae* isolate was regarded to be resistant to rifampicin, ofloxacin, sparfloxacin, as well as the low and intermediate levels of dapsone, but susceptible to clarithromycin and clofazimine.

Sequence analysis of the genes in the *M. leprae* isolate revealed mutations in *folP* at codon 55 (CCC→TCC), in *rpoβ* at codon 531 (TCG→TTC), and in *gyrA* at codon 91 (GCA→GTA). These mutations have been shown to be associated with dapsone-, rifampicin-, and quinolone-resistance, respectively in *M. leprae*.

The results clearly revealed the correlation between relevant mutations and drug resistance to each drug detected by the mouse footpad method. Previous reports have shown that the mutation at codon 55 in *folP* is a substitution of leucine for proline in high-level dapsone resistant strains ([7, 8]). Therefore, the missense mutation we observed (proline to serine) at codon 55 in the multidrug resistant *M. leprae* studied suggests resultant dapsone resistance at the intermediate level.

This is the fourth case of *M. leprae* resistance to multiple drugs used to treat leprosy. Single, or in a few instances, multidrug-resistant *M. leprae* have been detected among patients who have experienced clinical relapse ([1, 8, 9]). This has not been the case for patients treated with current World Health Organization (WHO)-recommended MDT. Standardized MDT regimens were not applied to Japanese patients before 2000 ([4]). The relapse patient reported in our study had been treated irregularly with several anti-leprosy drugs, suggesting drug resistance was a result of inadequate therapy.

The results of our study strongly support the use of drug resistance monitoring in relapse cases, and demonstrate the utility of drug susceptibility testing by gene mutation analysis. Ideally, gene mutation analysis for drug resistance should be applied when there is suspicion of drug resistance in leprosy. However, this approach is applicable to only three drugs at present. Early detection of drug resistant *M. leprae* will clarify treatment options and thereby curtail transmission of drug resistant bacilli. Also, we consider it important to begin to establish current levels of drug resistance by surveying leprosy patients for drug resistance using existing molecular tests, as well as developing new methods for detecting drug resistance to current and new drugs that may be useful for treating leprosy.

Acknowledgment. We would like to thank Thomas P. Gillis, National Hansen's Disease Programs, Baton Rouge, LA, USA for his thoughtful ideas for text alterations and consultation regarding this publication. This study was supported by a Health Research Grant of Emerging and Re-emerging Infectious Diseases, Ministry of Health, Labor and Welfare, Government of Japan and US-Japan Cooperative Medical Science Program.

REFERENCES

1. CAMBAU, E., BONNAFOUS P., PERANI E., SOUGAKOFF, W., JI, B., and JARLIER V. Molecular detection of rifampin and ofloxacin resistance for patients who experience relapse of multibacillary leprosy. Clin. Infect. Dis. **34** (2002) 39–45.
2. CAMBAU, E., PERANI, E., GUILLEMIN, I., JAMET, P., and JI, B. Multidrug-resitance to dapsone, rifampicin, and ofloxacin in *Mycobacterium leprae*. Lancet **349** (1997) 103–104.
3. DE WIT, M. Y. L., FABER, W. R., KRIEG, S. R., DOUGLAS, J. T., LUCAS, S. B., MONTREEWASUWAT, N., PATTYN, S. R. N., HUSSAIN, R., PONNIGHAUS, J. M., HARTSKEEL, R. A., and KLASTER, P. R. Application of polymerase chain reaction for the detection of *Mycobacterium leprae* in skin tissue. J. Clin. Microbiol. **29** (1991) 906–910.
4. GOTO, M., ISHIDA Y., GIDOH, M., NAGAO, E., NAMISATO, M., ISHII, N., and OZAKI, M. Guideline for the treatment of Hansen's Disease in Japan. (in Japanese) Jpn. J. Lepr. **69** (2000) 157–177.
5. GROSSET, J. H., GUEPLA-LAURAS, C.-C., BOBIN, P., BRUCKER, G., CARTEL, J.-L., CONSTANT-DESPORTES, M., FLAGEUL, B., FREDERIC, M., GUILLAUME, J.-C., and MILLAN, J. Study of 39 documented relapses of multibacillary leprosy after treatment with rifampin. Int. J. Lepr. Other Mycobact. Dis. **57** (1989) 607–614.
6. JACOBSON, R. R., and HASTINGS, R. C. Rifampin-resistant leprosy. (Letter) Lancet **2** (1976) 1304–1305.
7. KAI, M., MATSUOKA, M., NAKATA, N., MAEDA, S., GIDOH, M., MAEDA, Y., HASHIMOTO, K., KOBAYASHI, K., and KASHIWABARA, Y. Diaminodiphenyl sulphone resistance of *Mycobacterium leprae* due to mutations in the dehydropteroate synthase gene. FEMS Microbiol. Lett. **177** (1999) 231–235.
8. MAEDA, S., MATSUOKA, M., NAKATA, N., KAI, M., MAEDA, Y., HASHIMOTO, K., KIMURA, H., KOBAYASHI, K., and KASHIWABARA, Y. Multidrug resistant *Mycobacterium leprae* from patients with leprosy. Antmicrob. Agents Chemother. **45** (2001) 3635–3639.
9. MATSUOKA, M., KASHIWABARA, Y., and NAMISATO, Y. A *Mycobacterium leprae* isolate resistant to dapson, rifampicin, ofloxacine, and sparfloxacin. Int. J. Lepr. Other Mycobact. Dis. **68** (2000) 452–455.
10. PEARSON, J. M. H., REES, R. J. W., and WATERS, M. F. R. Sulphone resistance in leprosy. A review of one hundred proven clinical cases. Lancet **2** (1977) 69–72.

11. PETTIT, J. H. S., and REES, R. J. W. Sulphone resistance in leprosy. An experimental and clinical study. Lancet **2** (1964) 673–674.
12. SHEPARD, C. C., and MCRAE, D. H. A method for counting acid-fast bacteria. Int. J. Lepr. Other Mycobact. Dis. **36** (1968) 78–82.
13. SHETTY, V. P., UPLEKAR, M. W., and ANTIA, N. H. Primary resistance to single and multiple drugs in leprosy—a mouse footpad study. Lepr. Rev. **67** (1996) 280–286.

CLINICAL AND DIAGNOSTIC LABORATORY IMMUNOLOGY, Sept. 2003, p. 808–812 Vol. 10, No. 5
1071-412X/03/$08.00+0 DOI: 10.1128/CDLI.10.5.808–812.2003

Effect of Bacterial Flora on Postimmunization Gastritis following Oral Vaccination of Mice with *Helicobacter pylori* Heat Shock Protein 60

Hiroyuki Yamaguchi,[1]* Takako Osaki,[1] Haruhiko Taguchi,[1] Noriko Sato,[2] Atushi Toyoda,[1] Motomichi Takahashi,[1] Masanori Kai,[3] Noboru Nakata,[3] Akio Komatsu,[4] Yutaka Atomi,[2] and Shigeru Kamiya[1]

Department of Infectious Disease, Division of Medical Microbiology,[1] and First Surgery,[2] Kyorin University School of Medicine, Mitaka-shi, Department of Microbiology, Leprosy Research Center National Institute of Infectious Diseases, Higashimurayama-shi,[3] and Jiseikai Hospital, Suginami-ku,[4] Tokyo, Japan

Received 13 January 2003/Returned for modification 30 April 2003/Accepted 2 June 2003

In order to assess the efficacy of oral *Helicobacter pylori* heat shock protein 60 (HSP60) as a vaccine, protection against *H. pylori* infection in specific-pathogen-free (SPF) C57BL/6 and germfree (GF) IQI mice was examined. Prophylactic oral vaccination of these two strains of mice with either *H. pylori* HSP60 or *Escherichia coli* GroEL inhibited *H. pylori* colonization by 90 to 95% at 3 weeks postinfection (p.i.). However, these mice were only partially protected because bacterial loads increased in all animals at 10 weeks p.i. Anti-*H. pylori* HSP60 immunoglobulin G was detected in serum at 3 weeks p.i. in mice vaccinated with either *H. pylori* HSP60 or GroEL. Significant increases in the gastritis scores were observed only in SPF mice immunized with *H. pylori* HSP60. These results indicate that oral vaccination with *H. pylori* HSP60 has partial protective effects on subsequent *H. pylori* infection but also induces postimmunization gastritis. However, GF mice immunized with *H. pylori* HSP60 did not suffer from severe gastritis. Therefore, the presence of bacterial flora appears to contribute to the induction of postimmunization gastritis.

Helicobacter pylori infection is associated with the occurrence of chronic gastritis and is implicated in causing peptic ulcer diseases and gastric malignancies, such as mucosa-associated B-cell lymphoma and adenocarcinoma of the stomach (2, 11, 28, 39). This organism was recently categorized in carcinogen group I by the World Health Organization (17). Although serological studies have shown *H. pylori* infection in approximately half of the world's population, it is not clear how this pathogen persists in the stomach.

Eradication of chronic *H. pylori* infection with antibiotics obviously influences treatment for gastroduodenal diseases and reduces clinical symptoms. However, several problems are associated with antimicrobial therapy, including its side effects, as well as the generation of resistant strains of *H. pylori* (19, 25). Therefore, the development of a prophylactic vaccine would be an attractive strategy against *H. pylori* infection. Although the use of crude or purified *H. pylori* antigens has been explored in several animal models for the induction of protective immunity against *Helicobacter* species, these efforts have not resulted in the development of an optimal vaccine (20, 21, 26).

H. pylori heat shock protein 60 (HSP60) is known to be well conserved among different bacterial strains and is a strong immunogen (36, 38). Our previous studies showed that *H. pylori* HSP60, located on the bacterial surface, was involved in adhesion to gastric epithelial cells (35, 36). Moreover, Ferrero et al. have reported that vaccination with *H. pylori* HSP60 reduced colonization by *H. felis* in mice (9). Thus, these findings imply that *H. pylori* HSP60 has the potential to induce protective immunity against *H. pylori* infection.

In the present study, the efficacy of *H. pylori* HSP60 as an oral vaccine against *H. pylori* infection was assessed both in specific-pathogen-free (SPF) C57BL/6 and germfree (GF) IQI mice.

MATERIALS AND METHODS

Bacterial strains and preparation of antigens. *H. pylori* clinical isolate 1402 (*vacA*$^+$ *cagA*$^+$), obtained from a patient with gastritis, was used. *H. pylori* clinical isolate TK1029 (*vacA*$^+$ *cagA*$^+$), obtained from a patient with gastric ulcer, was used for the amplification of the *hsp60* gene and for the preparation of native *H. pylori* HSP60 by affinity purification methods described previously (34). *E. coli* pop2136 was used for the amplification of the *groEL* gene and for the transformation of expression plasmid pEX, which is capable of producing a β-galactosidase fusion protein (32). Construction of the *E. coli* expressing fusion proteins and the preparation of recombinant fusion protein was done by previously described methods (34, 37). cDNA fragments encoding *E. coli* GroEL and *H. pylori* HSP60 were amplified by PCR with the following primer sets: upstream for *E. coli groEL*, 5′-GAA TTC ATG GCA GCT AAA GAC GTA AA-3′; for *H. pylori hsp60*, 5′-GAA TTC ATG GCA AAA GAA ATC AAA TT-3′; and downstream for both genes, 5′-GAA TTC TTA CAT CAT GCC GCC CTA GC-3′. The GAATTC sites recognized by the *Eco*RI enzyme were added to both 5′ and 3′ sides for subcloning into the plasmid. All sequences of the amplified cDNAs inserted into the plasmid were confirmed by direct sequencing. These plasmids were then used to transform *E. coli* pop2136. The bacteria were cultivated at 30°C and shifted to 42°C for 2 h to induce the expression of the recombinant fusion proteins. Each transformed *E. coli* clone was disrupted by sonication (SONIFER 250; Bronson Ultrasonics Corp., Danbury, Conn.), and the insoluble fractions were collected. The pellet was incubated in 50 mM Tris-HCl (pH 8.0) containing 1 mM EDTA, 1 mM dithiothreitol, and 8 M urea for 1 h at 37°C. After the fusion proteins had been dialyzed against phosphate-buffered saline (PBS) and sterilized by filtration, they were applied as antigens for oral vaccination of mice against *H. pylori* infection. The fusion antigens containing *E. coli* GroEL and *H. pylori* HSP60 were designated rGalEcGroEL and rGalHpHSP60, respectively. The extract from *E. coli* transformed with pEX only was used as a control (rGal).

* Corresponding author. Mailing address: Department of Infectious Disease, Division of Medical Microbiology, Kyorin University School of Medicine, Mitaka, Tokyo 181-8611, Japan. Phone: 81-422-47-5511, x3464. Fax: 81-422-44-7325. E-mail: hiroyuki@kyorin-u.ac.jp.

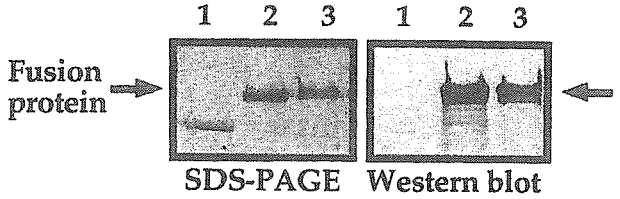

FIG. 1. Profiles of fusion protein on SDS-PAGE (left panel) and Western blot analysis with H9 MAb (right panel). A 1-μg portion of rGal (lane 1), rGalHpGroEL (lane 2), or rGalEcGroEL (lane 3) was loaded in each lane.

SDS-PAGE and Western blotting. Sodium dodecyl sulfate-polyacrylamide gel electrophoresis (SDS-PAGE) and Western blotting were carried out according to the methods previously described (34). Mouse monoclonal antibody (MAb) H9 (immunoglobulin G2a [IgG2a]), cross-reacting with *E. coli* GroEL and *H. pylori* HSP60 (34), was used as the fusion protein to detect antibody in Western blotting analyses.

Animal experiments. SPF C57BL/6 and GF IQI mice (both female, 6 weeks old) were purchased from Nipon CLEA (Tokyo, Japan). SPF and GF mice were housed under SPF conditions and in a sterilized isolator, respectively. Each group of mice (SPF [n = 20] and GF [n = 14]) was orally inoculated five times on a weekly schedule with 100 μg of recombinant antigen (rGal, rGalEcGroEL, or rGalHpHSP60) and 5 μg of heat-inactivated cholera toxin (CT; Sigma, St. Louis, Mo.) as a mucosal adjuvant or CT alone in 500 μl of PBS. After the last inoculation, 500 μl of *H. pylori* TK1402 (5×10^9 CFU/ml) was inoculated orally three times on a daily schedule.

Assessment of gastric inflammation. At 3 and 10 weeks after the final inoculation with *H. pylori*, mice were sacrificed, blood was collected for measurement of anti-*H. pylori* HSP60 IgG levels in serum, and stomachs were removed for determination of the number of *H. pylori* colonies and for the histological assessment of gastritis scores. The stomachs were washed in sterile PBS and cut longitudinally into two pieces: one half for bacterial cultures and the other half for histology. Longitudinal sections of gastric tissues from the esophageal-cardial junction to the duodenum were fixed in neutral 10% buffered formalin and embedded in paraffin. Sections of 4 μm thickness were stained with hematoxylin and eosin and viewed at magnifications of ×100 to ×400. Two histologists independently examined the gastric sections in a blind fashion. Gastritis was scored according to the method described by Dubois et al. (6) as follows: 0, intact mucosal lining and no infiltration of the lamina propria with mononuclear and polymorphonuclear cells; 1, mild increase of mononuclear or polymorphonuclear cell infiltration localized to the upper half of the mucosa; 2, mononuclear and polymorphonuclear cell infiltration extending from the surface into the lamina propria; and 3, either marked mononuclear and polymorphonuclear cell infiltration extending from the surface into the lamina propria or surface erosion.

Assessment of *H. pylori* in gastric tissue. Gastric mucosa (width, 3 mm; thickness, 0.5 mm) was suspended in Hanks balanced salt solution (Nikken Seibutu, Tokyo, Japan), by vortexing the sample until the mucosa was disrupted, and then plated on M-BHI PYLORI agar (Nikken Seibutu), a selective agar medium. After cultivation for 4 days at 37°C under microaerophilic conditions, gold-colored colonies were counted.

Determination of antibody levels against *H. pylori HSP60*. Enzyme-linked immunosorbent assay (ELISA) was performed as previously reported (34). Briefly, microplates were coated with affinity-purified *H. pylori* HSP60 and blocked with 1% skim milk–PBS. Mouse serum diluted 1:25 was added and visualized with goat anti-mouse IgG peroxidase conjugate (Cappel Research, Durham, N.C.) and OPD buffer (pH 5.0; 0.1 M citric acid, 0.07 M sodium phosphate dibasic 12-hydrate, and 0.015% [vol/vol] H_2O_2).

Statistical methods. Statistical significance for the differences between groups was assessed by using the Student t test.

RESULTS

Effect of oral vaccination against *H. pylori* infection. As shown in Fig. 1, H9 MAb reacted with a band of approximately 180 kDa in the fusion protein preparation. We first examined colonization of *H. pylori* in the stomach after vaccination. As shown in Fig. 2, oral vaccination with either rGalEcGroEL or rGalHpHSP60 significantly inhibited *H. pylori* colonization in the stomachs of both strains of mice by 3 weeks after infection. Compared to the control rGal-inoculated mice, vaccination resulted in reduction of infection by 90 to 95%. However, at 10 weeks postinfection (p.i.), the bacterial loads in both strains of mice were similar to the control CT group, regardless of which vaccine had been applied (data not shown).

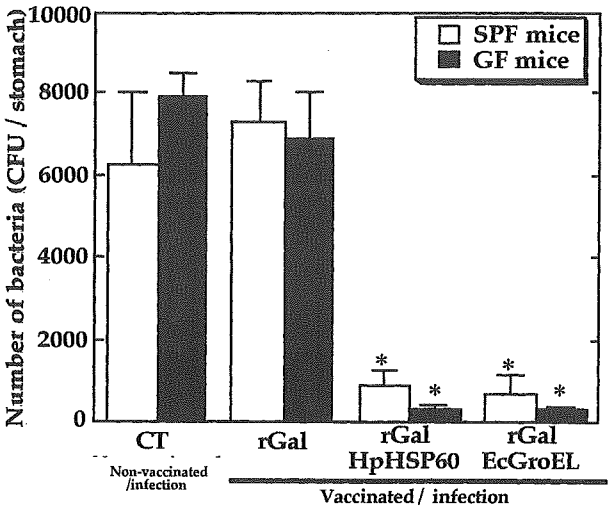

FIG. 2. Effect of vaccination on bacterial colonization in SPF and GF mice at 3 weeks p.i. The number of bacteria per stomach was determined by a bacterial culturing system as described in the text. The data represent the means plus the standard deviations for 10 (SPF) or 7 (GF) mice. *, $P < 0.05$ (i.e., significantly different from the control CT group [Non-vaccinated/infection]).

***H. pylori* HSP60-specific antibody levels in sera.** As shown in Table 1, elevated levels of IgG in serum against *H. pylori* HSP60 were present at 3 weeks p.i. in both SPF and GF mice vaccinated with either rGalEcGroEL or rGalHpHSP60. There were no significant differences between any of these groups. At 10 weeks after infection, there were still no significant differences among the groups (average ELISA values against *H. pylori* HSP60, 0.241 [SPF] versus 0.304 [GF]). The levels of IgG in serum were similar in all groups of infected mice, as well as controls (data not shown).

Histological examination of gastric tissue. It is known that after infection, previous oral vaccination frequently results in

TABLE 1. IgG response to purified *H. pylori* HSP60 in sera of SPF and GF mice

Group	Mean ELISA value (OD_{490})[a] ± SD in:	
	SPF mice	GF mice
Nonvaccinated with infection (CT only)	0.145 ± 0.041	0.234 ± 0.091
Vaccinated with infection		
rGal	0.286 ± 0.028	0.261 ± 0.022
rGalHpHSP60	0.521 ± 0.081[b]	0.552 ± 0.063[b]
rGalEcGroEL	0.651 ± 0.122[b]	0.566 ± 0.063[b]

[a] Data represent the mean values for each group at 3 weeks p.i. (SPF mice, n = 10; GF mice, n = 7). OD_{490}, optical density at 490 nm.
[b] $P < 0.05$ (versus the CT group animals).

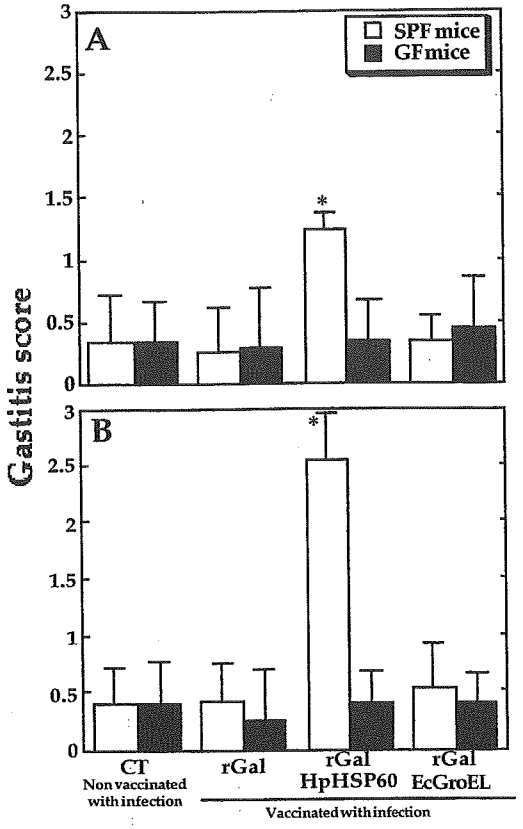

FIG. 3. Gastritis scores in vaccinated SPF and GF mice at 3 (A) and 10 (B) weeks p.i. Hematoxylin-eosin-stained gastric sections were scored for grade of inflammation (grades 0 to 3) as described in the text. The data represent the means plus the standard deviations for 10 (SPF) or 7 (GF) mice. *, $P < 0.05$ (i.e., significantly different from the control CT group [Nonvaccinated with infection]).

postimmunization gastritis (10, 12, 30). Therefore, we assessed whether *H. pylori* infection after oral vaccination causes gastric inflammation in these mice. As shown in Fig. 3, mild and severe gastritis was observed only in SPF mice preimmunized with rGalHpHSP60, at 3 and 10 weeks p.i., compared to the other groups. Furthermore, no significant increase of the gastric inflammation score was observed in any GF mice for up to 10 weeks p.i. Figure 4 shows representative photomicrographs of gastric tissues of rGalHpHSP60-vaccinated SPF and GF mice at 10 weeks p.i. Severe gastritis disrupting the glandular structure, surface erosion, and marked inflammatory cell infiltration was frequently observed in the SPF mice vaccinated with rGalHpHSP60 (Fig. 4A to C). However, the same vaccination with rGalHpHSP60 did not cause gastric inflammation in GF mice (Fig. 4D to F). Oral vaccination with rGalEcGroEL and a after infection also did not cause any severe gastric inflammation in either group of mice up to 10 weeks p.i. No inflammatory cell infiltration was observed in the stomachs of immunized mice without *H. pylori* infection up to 12 weeks after the last vaccination (data not shown). This finding suggests that *H. pylori* HSP60 immunization does not have any harmful effects per se. *H. pylori* infection alone without any other treatment caused inflammatory cell infiltration in either strain, similar to mice immunized with CT, rGal, or rGalEcGroEL (data not shown). In addition, none of the mice showed any atrophic changes (data not shown).

DISCUSSION

Our results showed that oral vaccination with *H. pylori* HSP60 or GroEL reduced subsequent bacterial colonization 3 weeks after *H. pylori* infection. However, these protective effects were transient, with the bacterial load recovering by 10 weeks p.i. Several previous studies had shown that oral vaccination with *H. pylori*-derived antigens, including *H. pylori* whole-antigen or purified antigen, together with an appropriate adjuvant such as CT, have at least partial protective effects, reducing or eliminating colonization of *H. pylori* in animal models. These protective effects in vaccinated mice can be of extended duration (9, 10, 12, 20, 21, 30). Although the reason for the difference between the present results and these earlier findings is still not clear, the decreasing *H. pylori* HSP60-specific IgG levels in serum at 10 weeks p.i. might be associated with transient protection. It may also be speculated that the extent of bacterial load depends on the kind of vaccine.

The bacterial loads in both strains of mice recovered by 10 weeks p.i., despite prior vaccination. It is known that Th2 immune responses are dominant in *H. pylori* infection, and have a potentially protective role for bacterial infection (5, 22, 33). In this regard, several reports showed that Th2 immune responses lead to an increase in the number of *H. pylori* colonies in the stomach (4, 23, 30). These findings seem to be a possible explanation for increased bacterial load in mice vaccinated with *E. coli* GroEL. However, it is still not clear how the bacterial load increased in mice immunized with *H. pylori* HSP60 and GroEL.

In SPF mice vaccinated with *H. pylori* HSP60, severe gastric inflammation, including erosion, was observed 10 weeks p.i. However, these findings did not apply in SPF mice vaccinated with *E. coli* GroEL. Thus, the results indicated that the postimmunization gastritis caused by *H. pylori* HSP60 was an antigen-specific phenomenon. A number of investigators have also reported that gastric inflammation occurs in immunized mice after challenge (postimmunization gastritis) (10, 12, 30). However, the mechanism by which vaccination induces gastritis is still not understood. In the present study, GF mice lacking normal bacterial flora did not show gastric inflammation. Therefore, the presence of bacterial flora seems to be important for the induction of postimmunization gastritis in the *H. pylori* vaccination mouse model. However, the SPF and GF mice used here belonged to different strains, which may also have accounted for the differences.

Numerous studies indicate that alterations of bacterial flora relate to critical inflammatory illnesses through the stimulation of the immune system (1, 24, 31). Interestingly, vaccinated GF piglets suffered only slight gastritis without erosion after *H. pylori* infection (8). Eaton et al. recently reported that immunodeficient SCID mice permit higher levels of *H. pylori* colonization and fail to develop gastritis compared to wild-type mice, suggesting that the host gastric inflammatory response is mediated by lymphocytes stimulated through gut-associated lymph nodes and not via direct bacterial contact (7). In the present study, we also showed that GF mice exhibit only a few inflammatory changes without erosion and atrophy after *H.*

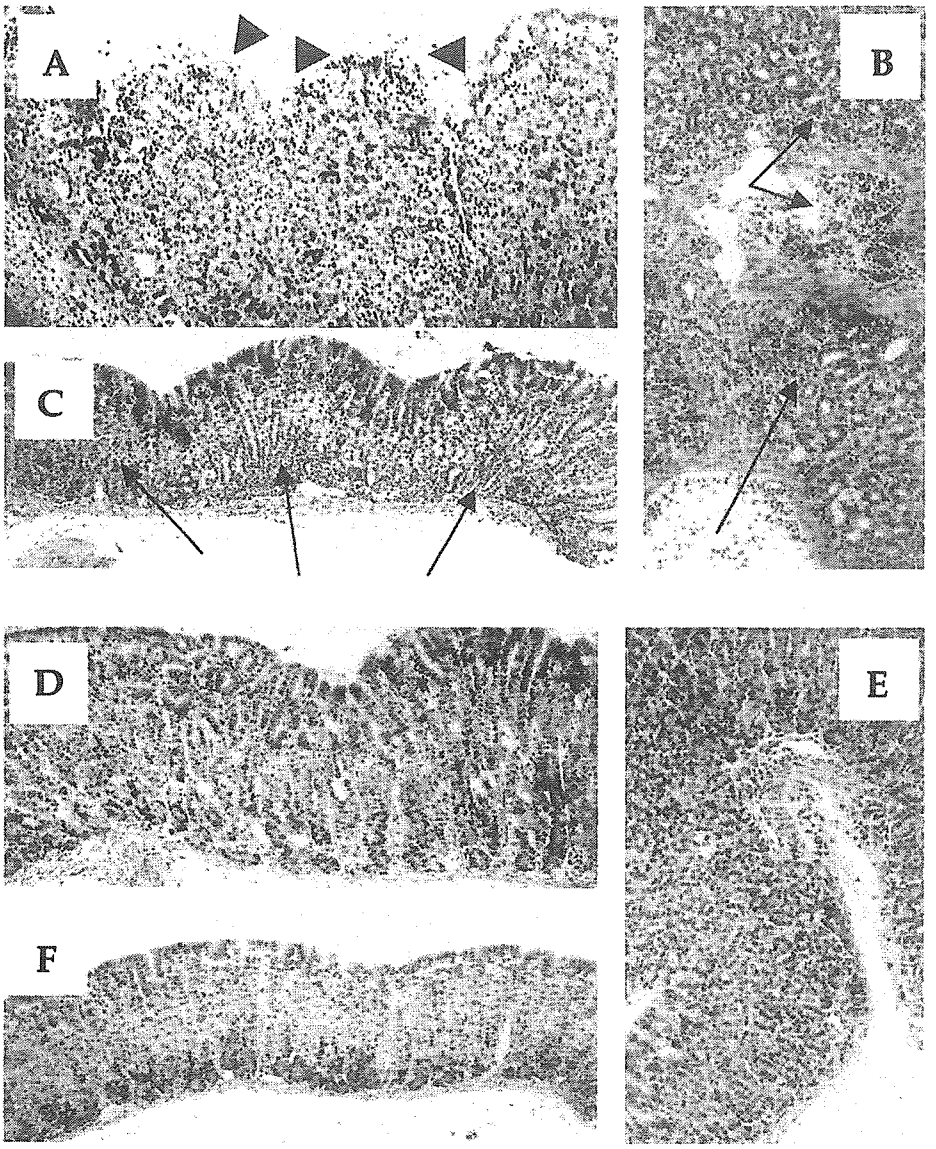

FIG. 4. Photomicrographs of hematoxylin-eosin-stained gastric tissues of SPF (A, B, and C) and GF (D, E, and F) mice prevaccinated with *H. pylori* HSP60 at 10 weeks p.i. Cardia mucosa of SPF mice frequently showed severe gastritis with disruption of the gland structure, severe inflammatory cell infiltration, and erosion (A). GF mice did not show these symptoms (D). Severe inflammatory cell infiltration was observed in mucosa in SPF mice (B) but not in GF mice (E). Antral mucosa of SPF mice also showed severe inflammatory cell infiltration (C), but GF mice did not (F). Arrows indicate inflammatory cell infiltration, and arrowheads indicate erosion. Magnification, ×200.

pylori challenge. Thus, these findings suggest that the signals to immune cells through intestinal bacterial flora after *H. pylori* infection might be responsible for the postimmunization gastritis. On the other hand, it is known that several receptors such as CD14, Toll-like receptors (TLRs), and CARD4 contribute to innate immune responses to bacterial pathogens in mucosal surfaces that constitute the first line of defense against microbial pathogens (3, 16, 18, 29). A recent study showed that upregulated stimulation through TLR2 and TLR4, which recognize bacterial cell wall components, is associated with the induction of intestinal inflammation (13). TLR5 was recently identified as the mediator of bacterial flagellin recognition and subsequent induction of innate immune responses (14). The upregulated stimulation via CARD4 was also associated with the induction of inflammatory bowel diseases, including Crohn's disease (15, 27). Although the reasons for such postimmunization gastritis in SPF mice are still unknown, it may be speculated that upregulated signaling to innate immunity through receptors stimulated by the combined intestinal bacterial flora, bacterial HSP60 antigen, and *H. pylori* might be important.

In summary, our data indicate that prophylactic immunization with *H. pylori* HSP60 results not only in a partial reduction of bacterial colonization but also in postimmunization gastritis in SPF mice. Because GF mice did not show this severe gastric inflammation, we conclude that the presence of bacterial flora might contribute to the induction of postimmunization gastritis after vaccination with *H. pylori* HSP60. Many questions remain

unanswered, including questions about the possible mechanisms of bacterial clearance and gastric inflammation caused by vaccination with *H. pylori* HSP60. However, the presence of bacterial flora may determine the usefulness and/or harmfulness of *H. pylori* HSP60 as a vaccine. The data in the present study might be valuable for the development of a vaccine for complete prevention of *H. pylori* without postimmunization gastritis.

ACKNOWLEDGMENT

We thank Catherine A. Newton (University of South Florida College of Medicine, Department of Medical Microbiology and Immunology) for careful reading and editing of the manuscript.

REFERENCES

1. **Bengmark, S.** 1998. Ecological control of the gastrointestinal tract: the role of probiotic flora. Gut **42:**2–7.
2. **Blaser, M. J., and J. Parsonnet.** 1994. Parasitism by the "slow" bacterium *Helicobacter pylori* leads to altered gastric homeostasis and neoplasia. J. Clin. Investig. **94:**4–8.
3. **Cario, E., I. M. Rosenberg, S. L. Brandwein, P. L. Beck, H. C. Reinecker, and D. K. Podoisky.** 2000. Lipopolysaccharide activates during signaling pathways in intestinal epithelial cell lines expressing Toll-like receptors. J. Immunol. **164:**443–451.
4. **Chen, W., D. Shu, and V. S. Chadwick.** 1999. *Helicobacter pylori* infection in interleukin-4-deficient and transgenic mice. Scand. J. Gastroenterol. **34:**987–992.
5. **Del Giudice, G., A. Covacci, J. L. Telford, C. Montecucco, and R. Rappuoli.** 2001. The design of vaccines against *Helicobacter pylori* and their development. Annu. Rev. Immunol. **19:**523–563.
6. **Dubois, A., C. K. Lee, N. Fiala, H. Kleanthous, P. T. Mehlman, and T. Monath.** 1998. Immunization against natural *Helicobacter pylori* infection in nonhuman primates. Infect. Immun. **66:**4340–4346.
7. **Eaton, K. A., S. R. Ringler, and S. J. Danon.** 1999. Murine splenocytes induce severe gastritis and delayed-type hypersensitivity and suppress bacterial colonization in *Helicobacter pylori*-infected SCID mice. Infect. Immun. **67:**4594–4602.
8. **Eaton, K. A., S. S. Ringler, and S. Krakowka.** 1998. Vaccination of gnotobiotic piglets against *Helicobacter pylori*. J. Infect. Dis. **178:**1399–1405.
9. **Ferrero, R. L., J. M. Thiberge, I. Kansau, N. Wuscher, M. Huerre, and A. Labigne.** 1995. The GroES homolog of *Helicobacter pylori* confers protective immunity against mucosal infection in mice. Proc. Natl. Acad. Sci. USA **92:**6499–6503.
10. **Garhart, C. A., R. W. Redline, J. G. Nedrud, and S. J. Czinn.** 2002. Clearance of *Helicobacter pylori* infection and resolution of postimmunization gastritis in a kinetic study of prophylactically immunized mice. Infect. Immun. **70:**3529–3538.
11. **Graham, D. Y., G. M. Lew, P. D. Klein, D. G. Evans, D. J. Evans, Jr., Z. A. Saeed, and H. M. Malaty.** 1992. Effect of treatment of *Helicobacter pylori* infection on the long-term recurrence of gastric and duodenal ulcers: a randomized controlled study. Ann. Intern. Med. **116:**705–708.
12. **Goto, T., A. Nishizono, T. Fujioka, J. Ikewaki, K. Mifune, and M. Nasu.** 1999. Local secretory immunoglobulin A and postimmunization gastritis correlate with protection against *Helicobacter pylori* infection after oral vaccination of mice. Infect. Immun. **67:**2531–2539.
13. **Hausmann, M., S. Kiessling, S. Mestermann, G. Webb, T. Spottl, T. Andus, J. Scholmerich, H. Herfarth, K. Ray, W. Falk, and G. Rogler.** 2002. Toll-like receptors 2 and 4 are upregulated during intestinal inflammation. Gastroenterology **122:**1987–2000.
14. **Hayashi, F., K. D. Smith, A. Ozinsky, T. R. Hawn, E. C. Yi, D. R. Goodlett, J. K. Eng, S. Akira, D. M. Underhill, and A. Aderem.** 2001. The innate immune response to bacterial flagellin is mediated by Toll-like receptor 5. Nature **410:**599–603.
15. **Hugot, J. P., M. Chamaillard, H. Zouali, S. Lesage, J. P. Cezard, J. Belaiche, S. Almer, C. Tysk, C. A. O'Morain, M. Gassull, V. Binder, Y. Finkel, A. Cortot, R. Modigliani, P. Laurent-Puig, C. Gower-Rousseau, J. Macry, J. F. Colombel, M. Sahbatou, and G. Thomas.** 2001. Association of NOD2 leucine-rich repeat variants with susceptibility to Crohn's disease. Nature **411:**599–603.
16. **Inohara, N., Y. Ogura, F. F. Chen, A. Muto, and G. Nunez.** 2001. Human Nod1 confers responsiveness to bacterial lipopolysaccharides. J. Biol. Chem. **276:**2551–2554.
17. **International Agency for Research on Cancer, World Health Organization.** 1994. Schistosomes, liver flukes, and *Helicobacter pylori*. Monogr. Eval. Carcinog. Risks Hum. **61:**218–220.
18. **Kopp, E. B., and R. Medzhitov.** 1999. The Toll-receptor family and control of innate immunity. Curr. Opin. Immunol. **11:**13–18.
19. **Lahaie, R. G., and C. Gaudreau.** 2000. *Helicobacter pylori* antibiotic resistance: trends over time. Can. J. Gastroenterol. **14:**895–899.
20. **Lee, A., and M. Chen.** 1994. Successful immunization against gastric infection with *Helicobacter* species: use of a cholera toxin B-subunit-whole-cell vaccine. Infect. Immun. **62:**3594–3597.
21. **Lee, C. K., R. Weltzin, W. D. Thomas, Jr., H. Kleanthous, T. H. Ermak, G. Soman, J. E. Hill, S. K. Ackerman, and T. P. Monath.** 1995. Oral immunization with recombinant *Helicobacter pylori* urease induces secretory IgA antibodies and protects mice from challenge with *Helicobacter felis*. J. Infect. Dis. **172:**161–171.
22. **Londono-Arcila, P., D. Freeman, H. Kleanthous, A. M. O'Dowd, S. Lewis, A. K. Turner, E. L. Rees, T. J. Tibbitts, J. Greenwood, T. P. Monath, and M. J. Darsley.** 2002. Attenuated *Salmonella enterica* serovar Typhi expressing urease effectively immunizes mice against *Helicobacter pylori* challenge as part of a heterologous mucosal priming-parenteral boosting vaccination regimen. Infect. Immun. **70:**5096–5106.
23. **Luzza, F., T. Parrello, L. Sebkova, L. Pensabene, M. Imeneo, M. Mancuso, A. M. La Vecchia, G. Monteleone, P. Strisciuglio, and F. Pallone.** 2001. Expression of proinflammatory and Th1 but not Th2 cytokines is enhanced in gastric mucosa of *Helicobacter pylori* infected children. Dig. Liver Dis. **33:**14–20.
24. **Marshall, J. C.** 1999. Gastrointestinal flora and its alterations in critical illness. Curr. Opin. Clin. Metab. Care. **2:**405–411.
25. **Megraud, F.** 1994. *H. pylori* resistance to antibiotics, p. 570–583. *In* R. H. Hunt and G. N. J. Tytgat (ed.), *Helicobacter pylori*: basic mechanism to clinical cure. Kluwer Academic Publishers, Dordecht, The Netherlands.
26. **Montgomery, M., S. Czinn, R. Redline, and J. Nedrud.** 1996. *Helicobacter*-specific cell mediated immune responses display a predominant Th1 phenotype and promote a delayed-type hypersensitivity response in the stomachs of mice. J. Immunol. **156:**4729–4738.
27. **Ogura, Y., D. K. Bonen, N. Inohara, D. L. Nicolae, F. F. Chen, R. Ramos, H. Britton, T. Moran, R. Karaliuskas, R. H. Duerr, J. P. Achkar, S. R. Brant, T. M. Bayless, B. S. Kirschner, S. B. Hanauer, G. Nunez, and J. H. Cho.** 2001. A frameshift mutation in NOD2 associated with susceptibility to Crohn's disease. Nature **411:**603–606.
28. **Peterson, W. L.** 1991. *Helicobacter pylori* and peptic ulcer disease. N. Engl. J. Med. **324:**1043–1048.
29. **Philpott, D. J., S. E. Girardin, and P. J. Sansonetti.** 2001. Innate immune responses of epithelial cells following infection with bacterial pathogens. Curr. Opin. Immunol. **13:**410–416.
30. **Raghavan, S., A. M. Svennerholm, and J. Holmgren.** 2002. Effects of oral vaccination and immunomodulation by cholera toxin on experimental *Helicobacter pylori* infection, reinfection, and gastritis. Infect. Immun. **70:**4621–4627.
31. **Romagnani, S.** 1999. Th1/Th2 cells. Inflamm. Bowel Dis. **5:**285–294.
32. **Stanly, K. K., and J. P. Luzio.** 1984. Construction of a new family of high efficiency bacterial expression vectors: identification of cDNA clones coding for human liver proteins. EMBO J. **3:**1429–1434.
33. **Smythies, L. E., K. B. Waites, J. R. Lindesy, P. R. Harris, P. Ghiara, and P. D. Smith.** 2000. *Helicobacter pylori*-induced mucosal inflammation is Th1 mediated and exacerbated in IL-4, but not IFN-γ, gene-deficient mice. J. Immunol. **165:**1022–1029.
34. **Yamaguchi, H., T. Osaki, M. Kai, H. Taguchi, and S. Kamiya.** 2000. Immune response against a cross-reactive epitope on the heat shock protein 60 homologue of *Helicobacter pylori*. Infect. Immun. **68:**3448–3454.
35. **Yamaguchi, H., T. Osaki, N. Kurihara, H. Taguchi, T. Yamamoto, and S. Kamiya.** 1997. Heat-shock protein 60 homologue of *Helicobacter pylori* is associated with adhesion of *H. pylori* to human gastric epithelial cells. J. Med. Microbiol. **46:**825–831.
36. **Yamaguchi, H., T. Osaki, H. Taguchi, T. Hanawa, T. Yamamoto, and S. Kamiya.** 1996. Flow-cytometric analysis of the heat shock protein 60 expressed on the cell surface of *Helicobacter pylori*. J. Med. Microbiol. **45:**270–277.
37. **Yasukawa, T., C. Kanei-Ishii, T. Maekawa, J. Fujimoto, T. Yamamoto, and S. Ishii.** 1995. Increase of solubility of foreign proteins in *Escherichia coli* by coproduction of the bacterial thioredoxin. J. Biol. Chem. **270:**25138–25231.
38. **Young, D. B.** 1990. Chaperonins and immune response. Semin. Cell Biol. **1:**27–35.
39. **Watanabe, T., M. Tada, H. Nagai, S. Sasaki, and M. Nakao.** 1998. *Helicobacter pylori* infection induces gastric cancer in Mongolian gerbils. Gastroenterology **115:**642–648.

特集I　微生物の免疫回避機構

らい菌と樹状細胞の相互作用*

牧野正彦**

Key Words：*Mycobacterium leprae*, DC, macrophage

はじめに

ハンセン病の原因菌であるらい菌は，1873年ノルウェーの医師Gerhard Henrik Armauer Hansenによって発見されたZiehl-Neelsen染色陽性の抗酸性桿菌である．芽胞や鞭毛は有さず，形態・性状が結核菌に類似するためgenus *mycobacterium*に分類されている．らい菌は，マクロファージと末梢神経シュワン細胞に強い親和性を示し，これらの細胞に感染したのち寄生性感染を果たし細胞内増殖をする．そのため，ハンセン病の主な病変は皮膚と末梢神経に出現し，臨床症状は感染部位に一致して出現する．とくに末梢神経障害は不可逆性であり，知覚神経と運動神経の両者が障害されるため，筋委縮や知覚神経麻痺による火傷・外傷を頻発し，その結果，著しい変形を伴う四肢機能障害が全身に出現する．それゆえに長い間，社会的偏見や差別の対象となってきた疾患である．

ハンセン病の病態病理，発症機構の解析，ワクチン開発，感染経路の解明など重要な課題が今なお未解決のままとり残されているが，その原因は，結核菌など他の抗酸菌と異なりらい菌は人工培養が不可能であること，末梢神経障害を誘導しうる動物モデルが存在しないことなどにある．また，らい菌とその他の抗酸菌とでは，菌の抗原性，生体防御反応誘導能など免疫学的観点において大きく異なっている．WHOはハンセン病の抑圧を目的として多剤併用化学療法(multidrug therapy：MDT)を導入し，登録患者数の著しい減少に成功した．しかし，全世界的には，今なお毎年数十万人にのぼる新患患者が発生していてワクチンの開発が切望されている[1]．さらに，近年薬剤耐性を示すらい菌が報告されるようになり[2]，化学療法に加える新たな治療法として免疫療法の開発が望まれている．ハンセン病に対するワクチンおよび免疫療法の開発には樹状細胞の果たす役割が大きい．ここではわれわれの最近の知見をもとに，らい菌と樹状細胞の相互作用について説明を加えたい．

樹状細胞のらい菌感受性と抗原提示能

ハンセン病は多彩な病型スペクトラムを呈する．WHOは多菌型(multibacillary：MB)と少菌型(paucibacillary：PB)の2型に分類することを推奨している．多菌型では，病変部位に抗酸性を示すらい菌が多数存在し，泡沫状を呈したマクロファージが数多く観察されるが，肉芽腫性病変は形成されない．病変は左右対称性にほぼ全身に広がる．一方，少菌型では，病変部位にらい菌が観察されることは稀で，活性化マクロファージが分化した類上皮細胞が中心となって肉芽腫

* Interaction of monocyte-derived dendritic cell with *mycobacterium leprae*.

** Masahiko MAKINO, M.D.: 国立感染症研究所ハンセン病研究センター病原微生物部〔〒189-0002 東村山市青葉町4-2-1〕; Department of Microbiology, Leprosy Research Center, National Institute of Infectious Diseases, Higashimurayama 189-0002, JAPAN

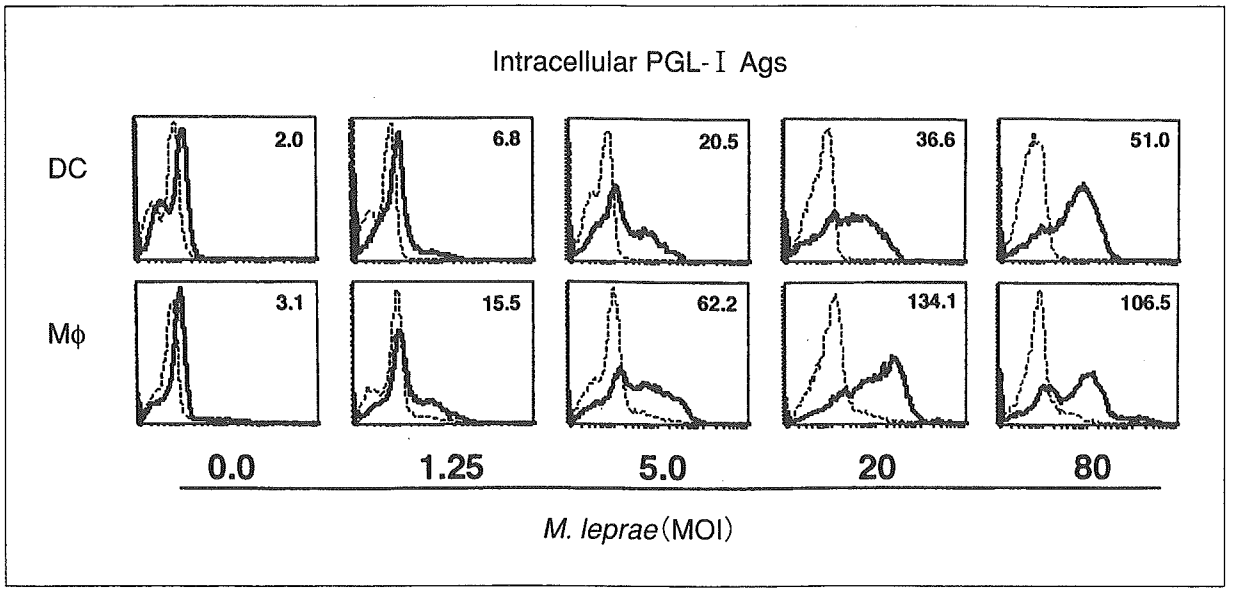

図1　細胞内PGL-I抗原の発現
樹状細胞とマクロファージを正常健常者末梢単球より誘導し，らい菌を感染させた．感染2日後に，細胞内PGL-I抗原の発現をFACS caliburを用いて検索した．点線：コントロール抗体，実線：抗PGL-I抗体．

性病変が形成される．病変部位は限局性散発性で，全身で1～2部位のみの病変を呈することもしばしばである．

多菌型と少菌型で観察されるらい菌に遺伝子構造上差はないため，同一の菌が異なった病型を誘導する．らい菌に対する細胞性免疫，とくにタイプ1細胞性免疫応答の強弱によって病型が規定されている．つまり，少菌型ではらい菌特異的なTh1タイプCD4陽性T細胞応答が誘導され，そのために菌は全身に拡がらず限局性病変を誘導する．一方，多菌型ではらい菌に対する細胞性免疫が作動せず(anergyが誘導されていることもある)，そのため菌は全身に拡がり，より重篤な病変を形成する．したがって，いかにしてらい菌に対する細胞性免疫を誘導するかが免疫療法およびワクチンの開発に重要となる．しかし，マクロファージに感染したらい菌は種々の方策を用いて，マクロファージのプロセッシング(processing)作用を抑制し，同時にライソゾーム(lysosome)との融合を阻止する．その結果，らい菌はファゴゾーム(phagosome)内に長期にわたりとどまり，寄生性感染を果たす．このような抑制機構としていくつかの機序が知られているが，その1つとしては，らい菌感染マクロファージのファゴゾームでは酸化機構が働かず，そのためにライソゾームとの融合が抑制されると考えられている[3]．また，マクロファージの細胞膜にはTACO(tryptophan aspartate-containing coat protein)が存在するが，らい菌が生きた状態でファゴゾームに取り込まれると，TACOが細胞膜からファゴゾーム膜へと局在を変化させ，ライソゾームとの融合を阻止する可能性も考察されている[4]．いずれにしてもファゴゾームに取り込まれたらい菌は，マクロファージのプロセッシングに関わる機構を阻害することにより，MHC分子へのペプチド付加を抑制し，ひいてはT細胞の活性化を阻止する．結果として宿主の生体防御能の活性化を抑制する．

一方，ヒト末梢血単球由来樹状細胞は，生体内におけるもっとも有能なprofessional抗原提示細胞として知られている．そのゆえんは，樹状細胞はnaive T細胞もmemory T細胞も活性化することが可能であり，さらに，外来性蛋白抗原の侵入あるいは細菌感染を受けた場合に，CD4陽性T細胞ばかりでなくCD8陽性T細胞をも賦活することが可能な点にある．これまでT細胞(とくにCD4陽性T細胞)が活性化されて産生するIFN-γが抗酸菌に対する生体防御としてもっとも有効な働きをすると考えられてきた[5]．IFN-γの作用については不明な点も多いが，らい菌感

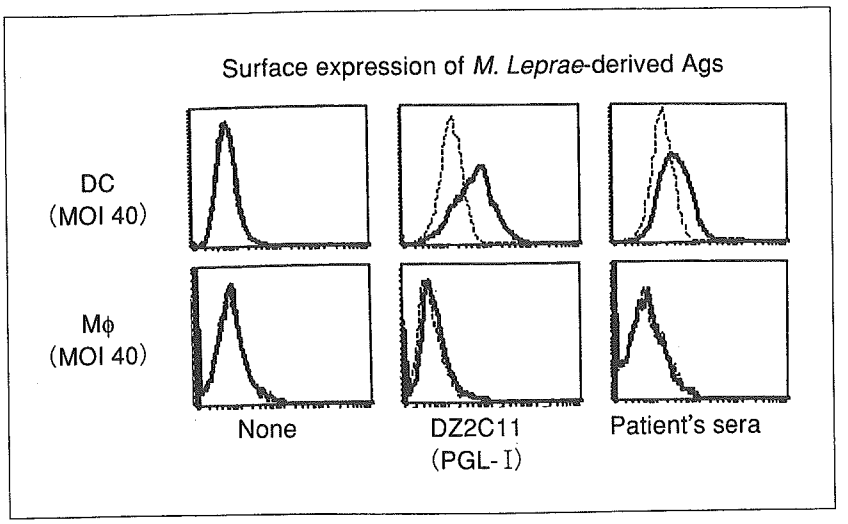

図2　らい菌由来抗原の樹状細胞およびマクロファージの細胞表面への発現
図1と同様にして細胞を作成し，らい菌を感染させた．感染2日後に細胞を抗PGL-I抗体とハンセン病患者血清を用いて染色した．点線：コントロール抗体あるいは正常健常者血清，実線：抗PGL-I抗体あるいは患者血清．

染したマクロファージを活性化させることで，細胞内に存在する菌を殺戮することが可能になると考えられている[6]．一方近年の研究において，CD4陽性T細胞ばかりでなくCD8陽性T細胞も抗抗酸菌生体防御反応ではきわめて重要な役割を果たすことが明らかにされている．この際CD8陽性T細胞は，perforinとgranulysinの両者を産生するcytotoxic T lymphocytes(CTL)に分化する必要がある[7]．Perforinはターゲット細胞の細胞膜の透過性を高め細胞を殺す役割を担い，granulysinは直接的に細胞内抗酸菌を殺戮する．したがって，CD4陽性およびCD8陽性T細胞の両者を活性化することが生体防御反応として重要であり，両T細胞の活性化のために必要な抗原提示細胞としては樹状細胞に大きな期待がかかる．しかし，生体内樹状細胞がらい菌に感染し，らい菌を細胞内に保持していることを証明した報告はきわめて少ない．

そこで*in vitro*において正常健常者末梢単球由来樹状細胞のらい菌に対する感受性を検討した[8]．樹状細胞にらい菌をパルスした後，抗酸菌染色を施すと，加えた菌の量に依存して細胞内に存在するらい菌の量が増加した．しかし，樹状細胞膜に付着して残存する菌は散見されなかった．感染した菌の量を半定量化する目的で，FACSを用い細胞内のPGL-I抗原(らい菌壁に存在するらい菌特異的抗原)を測定すると，加えた菌量に依存してPGL-I抗原の発現が増強した．また，その程度は感染マクロファージとほぼ同じであった(図1)．したがって，樹状細胞はらい菌に対して強い感受性を有すと想定された．一方，樹状細胞はマクロファージと異なり，らい菌感染を受けるとその細胞表面にPGL-I抗原およびハンセン病患者血清と反応する抗原を発現した(図2)．そこで，らい菌感染樹状細胞の抗原提示に関与する抗原の発現について検討すると，コントロールに用いた*M. bovis* BCG菌は樹状細胞のMHC class I, class IIおよびCD86抗原の発現を著しく増強させたにもかかわらず，らい菌ではむしろMHC class IおよびclassII抗原の発現を低下させた．CD86抗原は，大量の菌(MOI 160)を用い初めて強陽性となった．樹状細胞の活性化マーカーであるCD83抗原の発現にも大量の菌を要した(図3)．

ついで，抗酸菌感染樹状細胞の抗原提示能力を自己のCD4およびCD8陽性T細胞の増殖応答能(表1)あるいはIFN-γ産生能を指標として，らい菌とその他の抗酸菌(*M. bovis* BCG, *M. avium*)とを対比しつつ検討した．コントロールとして用いた抗酸菌が比較的少量の菌(MOI<1.0)でCD4陽性およびCD8陽性の強い増殖を誘導しIFN-γの産生をもたらしたにもかかわらず，らい菌ではMOI 40～160と大量の菌を用いた時のみT細胞を活性化(増殖とIFN-γ産生)した．こうした大量の菌を必要とする現象は，らい菌以外の抗酸菌